

Synergistic Prevention of Biofouling in Seawater Desalination by Zwitterionic Surfaces and Low-Level Chlorination

Rong Yang, Hongchul Jang, Roman Stocker,* and Karen K. Gleason*

Water scarcity affects one in three people in the world.^[1] With nearly 98% of the world's available water supply being seawater or brackish water, desalination has become an important means to address the scarcity of freshwater resources. Thin film composite (TFC) reverse osmosis (RO) membranes enable the removal of salt ions from seawater at room temperature by applying pressure to the seawater feed. TFC-RO has quickly become the dominating desalination method since its commercialization in the 1980s and is now used in nearly all RO desalination plants.^[2] TFC-RO is considered to have the greatest water permeability with high salt rejection rate.^[2] The bottleneck for TFC-RO to produce freshwater via seawater desalination at a comparable price to natural freshwater is severe membrane fouling, which impairs water permeation and salt rejection and thus reduces freshwater yield. Currently, marine biota and in particular bacteria are removed from the feed by pretreatment, the most energy-intensive (responsible for >36% of total plant energy consumption) and chemical-intensive step in a desalination plant and one that poses environmental risks to marine organisms when treated water is discharged back into the ocean.^[2] Fouling-resistant RO membranes would bring major improvements in energy usage, process reliability and lower the environmental impact of seawater desalination.

Zwitterions are a type of molecular structures with ultra-low fouling properties, demonstrated in applications ranging from bio-assays to artificial tissues,^[3,4] originating from the extreme hydrophilicity induced by electrostatic interaction with water molecules,^[5,6] which makes the replacement of surface-bound water molecules by foulants enthalpically unfavorable. However, the zwitterionic coatings fabricated so far are not sufficient in long-term antifouling applications due to the limited stability in real-world environments.^[7]

The major challenge in the surface modification of TFC-RO membranes is to implement antifouling chemistries without

compromising salt rejection and high water flux.^[2] The limiting step for the transport of water and salt across membranes is the extremely thin (~100 to 200 nm) polyamide selective layer (Figure 1a). Pin-holes or defects in the polyamide layer are routes for non-selective salt transport and thus quench the salt rejection performance of the membranes. Surface modification methods involving solvents or exposure to high temperatures (Table 1) can generate or enlarge the undesirable pin-hole defects.^[8] Surface modification layers produce an additional resistance to water permeability. We have shown previously that the coatings on RO membranes should be 30 nm or thinner and thicknesses >100 nm are undesirable because they cause >40% reduction in the water flux.^[9]

Recently, we showed that anti-biofouling coatings of various compositions can be grafted and directly deposited on commercial TFC-RO membranes via an all-dry process, called initiated chemical vapor deposition (iCVD).^[9-11] The low-temperature, solvent-free processing leaves the delicate polyamide intact and thus maintains the high salt rejection. Water flux is maintained by utilizing ultrathin (30 nm) iCVD layers. However, these acrylate-based films do not resist the degradation by chlorine, the most prevalent disinfection reagent in water treatment.^[12]

We report here a novel pyridine-based zwitterionic surface chemistry that displays significantly improved resistance against a variety of molecular foulants and improved tolerance to chlorine exposure as compared to acrylate-based analogues. The chlorine-resistant surface provides a new perspective for achieving long-term antifouling. The pyridine-based zwitterionic surfaces demonstrate a synergy with drinking-water-level chlorination (5 ppm), resulting in exceedingly high antifouling performance. Synergistic effects have often been observed in the interactions between pairs of molecules such as pairs of drugs or toxins, or pairs of surface properties, such as surface energy and roughness. However, to our knowledge, synergistic effects have not been specifically identified between a functional surface and a solution species. The chlorine-resistant antifouling surfaces are derived from ultrathin iCVD poly(4-vinylpyridine) (P4VP) and its copolymers.^[13,14] The vapor deposition allows the synthesis of insoluble cross-linked coatings as thin films directly on a surface in a single step. Enhanced durability results from cross-linking co-monomers and in situ grafting. The in situ reaction with 1,3-propanesultone (PS) vapors produces pyridine-based sulfobetaine zwitterionic functional groups, having a balanced surface charge. The iCVD synthesis is carried out at low surface temperature (20 °C) to produce robustly adhered, smooth, ultrathin layers (30 nm) directly on even delicate substrates, such as TFC-RO membranes without damaging them. Accelerated testing against marine

R. Yang, Prof. K. K. Gleason
Department of Chemical Engineering
Massachusetts Institute of Technology
77 Massachusetts Avenue, Cambridge
Massachusetts, 02139, USA
E-mail: kkg@mit.edu

Dr. H. Jang, Prof. R. Stocker
Ralph M. Parsons Laboratory
Department of Civil and Environmental Engineering
Massachusetts Institute of Technology
77 Massachusetts Avenue, Cambridge
Massachusetts, 02139, USA
E-mail: romans@mit.edu



DOI: 10.1002/adma.201304386

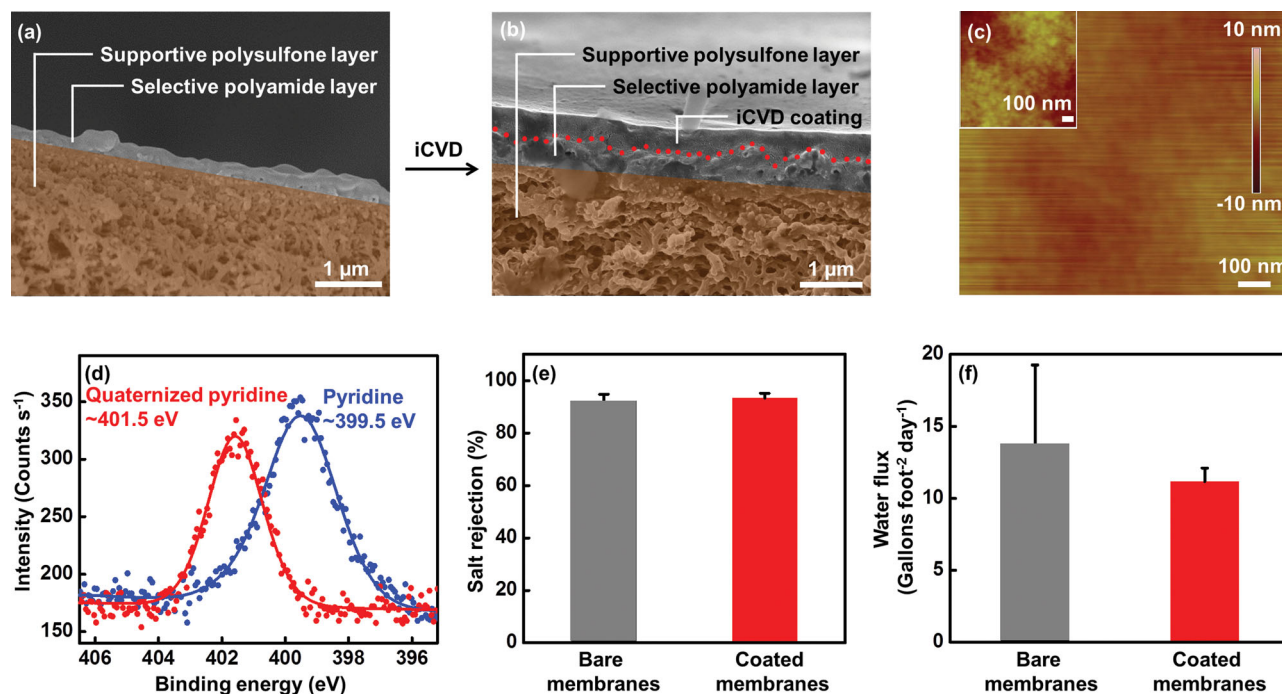


Figure 1. Antifouling zwitterionic coatings applied onto commercial RO membranes via iCVD. a,b) Cross-sectional SEM image of (a) bare and (b) iCVD coated RO membrane. Panel (a) shows the porous supportive polysulfone layer (colored in orange) beneath the nonporous, 200-nm-thick, selective polyamide layer of the RO membrane. In (b), the smooth top layer is the iCVD zwitterionic coating, which is grafted to the selective layer. c) AFM scan of coated membrane and (inset) bare membrane. Both surfaces are exceptionally smooth, with ~ 1 nm RMS roughness. d) N(1s) XPS high resolution scan of the iCVD P4VP as-deposited (blue) and derivatized by PS (red), demonstrating full conversion of pyridine to zwitterion. e) Salt rejection of bare and coated membranes. The comparable values of salt rejection indicate that the coating leaves the thin selective layer of the delicate RO membranes intact. f) Water flux through bare and coated membranes. Membranes coated with 30-nm functionalized copolymer 1 maintain 86% of the original water flux. Error bars (e,f) represent the standard deviations obtained with 3 parallel tests.

bacteria in multichannel microfluidic devices shows ~ 100 -fold reduction in biofouling on the coated surface compared to bare glass. The unique resistance of the pyridine-based films against degradation by chlorine allows a new synergistic approach to antifouling, which substantially enhances longer-term fouling resistance compared to either surface modification or chlorination alone, and has the potential to reduce or eliminate pretreatment of seawater, the most energy- and chemical-intensive step in desalination plants, and thus to reduce the cost of freshwater production and its collateral toxicity to marine biota. This approach can facilitate the rational design of the next

generation of RO membranes^[15–17] and of antifouling strategies in desalination plants, and find additional utility on the hulls of ships and for submerged marine structures.^[18]

Ultrathin (30 to 300 nm) iCVD coatings are successfully grafted and deposited directly onto commercial TFC-RO membranes (Figure 1b), followed by the vapor phase derivatization (Supporting Information, Figure S1). The all-dry-processed coating conforms to the geometry of the underlying substrate (Figure 1b,c), because surface tension and de-wetting are avoided. The root-mean-square (RMS) roughness of bare and coated RO membranes is 1.3 ± 0.3 nm (Figure 1c, inset) and

Table 1. Comparison of the important characteristics of surface modification techniques for zwitterionic antifouling chemistries.

Methods	SAMs ^[35]	Atom-transfer radical-polymerization ^[36]	Bulk solution polymerization ^[4]	Layer-by-layer ^[37]	iCVD
All-dry processing	X	X	X	X	V
Substrate-independence	X	X	V	X	V
Synthesis speed					
[nm min ⁻¹]	10 ⁻³	10 ⁻²	$\sim 10^3$	~ 1	~ 10
Small post-treatment roughness	V	V	X	X	V
Conformal coating	V	V	X	V	V
Ultra-thin coating	V	V	X	V	V
High surface concentration of zwitterionic groups	V	V	X	V	V

0.8±0.1 nm (Figure 1c), respectively. This exceptional smoothness is critical to the fouling resistance of the membrane surface,^[2] because larger surface areas and more binding sites are available for foulants to attach on a rougher surface. In addition, nano- and micro-scale roughness can entrap proteins and bacteria, respectively, and provide a “shield” to attached foulants from shear forces.^[19] The benign reaction conditions allow retention of the zwitterionic groups, as evidenced by the N(1s) high-resolution scan by X-ray photoelectron spectroscopy (XPS, Figure 1d). The binding energy of the pyridine nitrogen species in the as-deposited iCVD layer is ~399.5 eV^[20] with a small tail around 402 eV that is attributed to the inevitable post-treatment adsorption of atmospheric CO₂.^[21] The binding energy of quaternized pyridine nitrogen is ~401.5 eV^[21] and the symmetric peak profile indicates complete quaternization by the derivatization with PS.

The salt rejection of the surface-modified RO membranes is unaltered, confirming the benign nature of the solvent-free process (Figure 1e). This substrate-independent method allows simultaneous deposition on multiple substrates. This feature is used to simultaneously deposit on RO membranes and on a silicon wafer in order to achieve precise control of coating thickness, which is critical because thin coatings are essential to maintaining the high water flux through RO membranes.^[2] The coating thickness on RO membranes is compared to that on a silicon wafer,^[9] which is monitored via *in situ* interferometry. With the 30-nm coating thickness achieved by this method, the water flux is reduced only by ~14% compared to untreated RO membranes (Figure 1f). This high water flux is achieved with an amount of the cross-linker (4%; copolymer 1; Supporting Information, Figure S1), divinylbenzene (DVB), sufficiently high to ensure the stability of the coating and sufficiently low to effect a minimal reduction in water flux. As expected, water flux is reduced (by 72%; Supporting Information, Figure S2) for higher DVB content (17%; copolymer 2) and also (by 84%) for the homopolymer PDVB, owing to its high cross-linking density. It is worth noting that copolymer 1, despite the higher cross-linking density, has similar water flux as homopolymer P4VP (Supporting Information, Figures S1 and S2). This is likely a result of surface chain reorganization of copolymer 1 upon contacting water. Therefore, copolymer 1 is chosen as providing the optimal trade-off between coating stability and water flux. Taken together, these results show that the proposed approach can overcome the major challenge in the field of surface modification for desalination, by implementing antifouling chemistry without compromising water flux and salt rejection of the resulting membranes.

To reveal the chemistry of the antifouling coatings, the retention of functional groups and compositions of as-deposited and functionalized iCVD polymers are analyzed using Fourier transform infrared (FTIR). Excellent agreement is observed between the spectra of iCVD- and solution-polymerized PDVB and P4VP,^[22,23] indicating that the non-vinyl organic functionalities in the monomers are retained in the iCVD films. Successful polymerization of DVB (Figure 2b) is evidenced by the reduction of the 903 cm⁻¹ peak in the PDVB spectrum (Figure 2a, black), which results from the out-of-plane CH₂ deformation in vinyl groups. The existence of this peak in the PDVB spectrum is due to the presence of unreacted pendant vinyl

bonds.^[13,24] For the iCVD polymers PDVB (black), copolymer 2 (wine), copolymer 1 (magenta) and P4VP (blue), there is a decreasing trend in the area under the 710 cm⁻¹ peak, a measure of the number of *m*-substituted aromatic rings in the DVB repeat units (Figure 2a). This is utilized to calculate compositions of the iCVD copolymers,^[13] which are confirmed by XPS survey scans. The composition of the copolymers can be tuned simply by varying the flow rate ratios of 4VP and DVB monomers (Supporting Information, Figure S1). In the spectra of P4VP and copolymers, the strong peak at 1600 cm⁻¹ is attributed to the C-C and C-N stretching vibrations in the pyridine ring (Figure 2c),^[13,24] whose intensity increases with more P4VP repeat units (Supporting Information, Figure S1). FTIR spectra collected after the PS derivatization (Figures 2a and S1) confirms the formation of the pyridine-based sulfobetaine (Figure 2d) via ring-opening of PS, as evident by the appearance of a peak at 1036 cm⁻¹ in the spectra of functionalized P4VP (red) and copolymer 1 (orange) (Figure 2a). This peak is attributed to the symmetric stretching of the SO₃⁻ group.^[24] Therefore, pyridine-based zwitterionic structures designed to resist oxidative damages are successfully synthesized using the solvent-free scheme.

To evaluate the chlorine resistance of the iCVD films, we subject the functionalized homopolymer P4VP, copolymer 1 and copolymer 2 to treatment with a 1000 ppm solution of sodium hypochlorite and we acquire FTIR spectra after different treatment durations. From the spectra, we measure the areas under the 1600 cm⁻¹ peak (Figure 2a,e) to quantify the functional retention of the zwitterionic structure; the strong peak intensity renders the quantification more accurate. The excellent chlorine resistance of copolymer 1 (4% DVB) is evident from the negligible changes in its spectrum after 2 (green) and 24 (grey) hours of chlorine treatment (Figure 2a). In contrast, homopolymer P4VP is rendered soluble by a 10-hour exposure, as shown by the absence of functional peaks in the FTIR spectrum (Supporting Information, Figure S3). Importantly, the addition of 4% DVB cross-linker produces a major increase in the resistance to chlorine, whereas additions beyond 4% result in minor additional resistance (Figure 2e): after 10000 ppm h exposure to chlorine, ~94% and ~99% pyridine functionalities remain in functionalized copolymers 1 (4% DVB) and 2 (17% DVB), respectively. Functionalized copolymer 1 is thus most desirable because it resists chlorine very effectively while leaving the water flux nearly intact (Supporting Information, Figure S2).

These observations are corroborated by dynamic contact angle measurements on functionalized P4VP and copolymer 1 before and after chlorine treatment, which yields a comprehensive evaluation of the effects of chlorine on the coatings, because the dynamic contact angles of coated surfaces are affected by coating chemistry, surface roughness, swelling, and surface chain reorganization.^[25] For the functionalized P4VP, before chlorine treatment we measure advancing and receding contact angles of 31° and 20°, whereas after 2000 ppm h chlorine exposure these values become 48° and 18°, respectively (Supporting Information, Figure S4). These considerable changes in dynamic contact angles reflect the poor chlorine resistance of the functionalized P4VP films. In contrast, the advancing and receding contact angles of the functionalized copolymer 1 are 51° and 24°, respectively. In spite of the higher

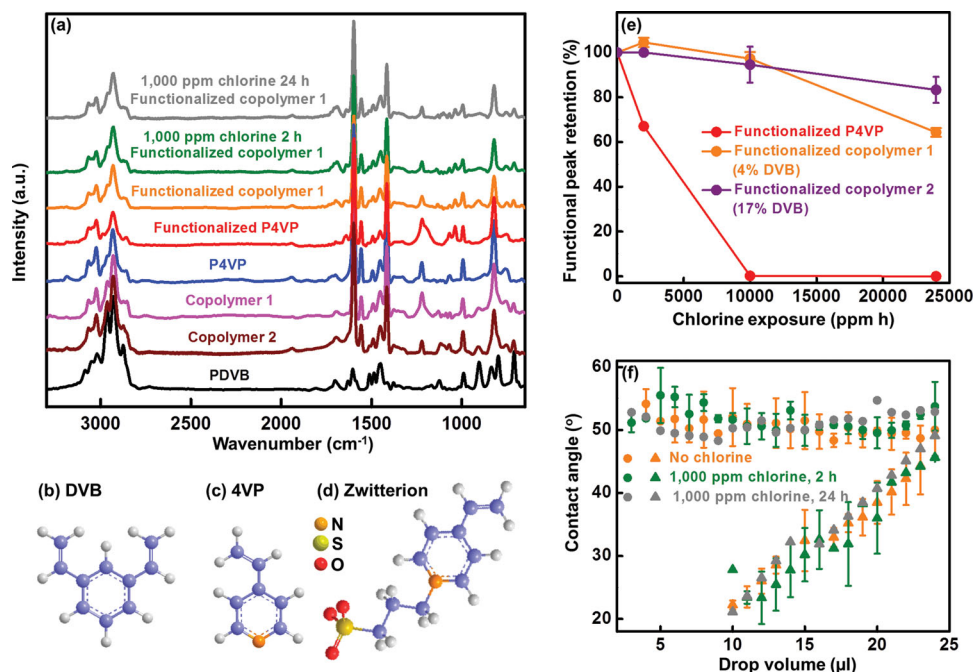


Figure 2. Chlorine-resistant zwitterionic chemistry. a) FTIR spectra of homopolymers and copolymers as-deposited, after PS functionalization, and after chlorine exposure. Copolymer 1 and 2 contain 4% and 17% DVB repeat units, respectively. The spectra of functionalized P4VP and copolymer 1 display a peak corresponding to the zwitterionic moiety (1036 cm⁻¹). Copolymer 1 shows unchanged spectra after 1000 ppm chlorine treatment for 2 hours and 24 hours, demonstrating excellent chlorine resistance. Spectra are offset vertically for clarity. b-d) Molecular structure of the cross-linker DVB, 4VP and the zwitterionic moiety obtained after functionalization. e) The polymers' chlorine resistance, quantified as the area under the 1600 cm⁻¹ peak (corresponding to the pyridine ring). Functionalized homopolymer P4VP does not resist the oxidative damage of chlorine, whereas functionalized copolymer 1, containing merely 4% cross-linker repeat units, resists chlorine considerably better. Increasing cross-linker repeat units beyond 4% improves chlorine resistance only slightly. f) Advancing (●) and receding (▲) contact angles of the functionalized copolymer 1 before and after chlorine treatment. The drop volume is the volume of the water droplet used to measure the contact angle. Contact angles are unchanged by chlorine treatment, confirming the chlorine resistance observed via FTIR (a).

cross-linking density, copolymer 1 has similar receding contact angle as P4VP. This is a sign of surface chain reorganization^[25] and corroborates the comparable water flux obtained with functionalized P4VP and copolymer 1 films. The dynamic contact angles remain unchanged after as much as 24000 ppm h chlorine treatment (Figure 2f), confirming the excellent chlorine resistance of the functionalized copolymer 1 films: the coating chemistry, surface roughness, swelling, and surface chain reorganization all remain essentially unaltered even upon prolonged exposure to chlorine.

We demonstrate the anti-biofouling properties of the new surface chemistry both with dissolved foulants and with marine bacteria. Quantification of the surface adsorption of 1 mg ml⁻¹ bovine serum albumin (BSA) in phosphate-buffered saline (PBS) is conducted via quartz crystal microbalance with dissipation monitoring (QCM-D). BSA is a widely used test protein for antifouling studies.^[26,27] Analogous tests are carried out with a representative polysaccharide, 1 mg ml⁻¹ sodium alginate, the major component of extracellular materials that lead to membrane biofouling.^[28] QCM-D tests reveal no adsorption of either foulant over 200 minutes on the functionalized copolymer 1 surface (Supporting Information, Figure S5). The thickness of the coating does not have an impact on the fouling resistance (Supporting Information, Figure S6), because the derivatization

with PS is diffusion-limited and the zwitterionic moieties are only present in the top few nanometers.^[10] The consistent fouling resistance under low (PBS buffer) and high (2 M NaCl added to PBS buffer, corresponding to ~117,000 ppm NaCl) salt concentrations implies that the functionalized copolymer 1 surface is charge-neutral (Figure S6).

The good fouling resistance against dissolved chemicals leads us to test the surfaces against fouling by marine bacteria. We use both natural seawater samples and a culture of *Vibrio cyclitrophicus*, a species broadly representative of bacteria prevalent in coastal waters, from where seawater for desalination typically originates. The dynamics of bacterial attachment are studied in a microfluidic flow system and imaged with an inverted microscope equipped with a CCD camera.^[29] Images are extracted from full movies (Supporting Information, Movies) and quantified by image analysis. Microchannels of 600 × 100 μm rectangular cross-section are fabricated out of polydimethylsiloxane (PDMS) using standard soft lithography techniques^[29] and mounted on a microscope glass slide that has been coated with a ~300-nm-thick film of functionalized copolymer 1. Fresh seawater is harvested and used on the same day as the feed solution for the microfluidic fouling tests, without any pretreatment, through continuous injection at a rate of 2 ml min⁻¹ (corresponding to a mean flow

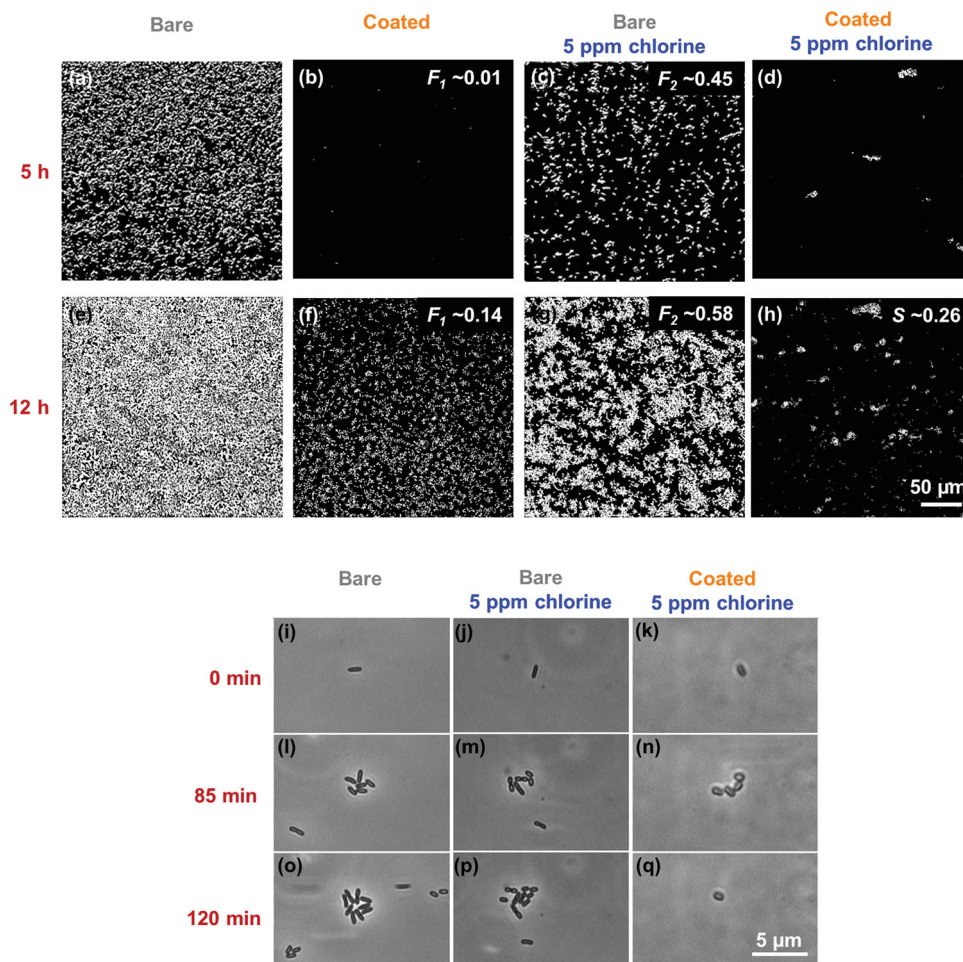


Figure 3. Enhanced fouling resistance by zwitterionic surfaces and low-level chlorination. a-h) Attachment of concentrated suspensions of the marine bacteria *V. cyclitrophicus* to glass surfaces with (a,e) no treatment; (b,f) the zwitterionic coating (functionalized copolymer 1); (c,g) chlorination (5 ppm); and (d,h) the zwitterionic coating plus chlorination, after 5 hours (a-d) and 12 hours (e-h). The zwitterionic coating shows no signs of fouling after 5 hours under accelerated biofouling tests conditions (b), whereas after the same amount of time the bare surface has significant surface coverage by bacteria (a). After 12 hours, neither the coating alone (f) nor chlorination alone (g) is effective at resisting biofouling, whereas the combined treatment exhibits dramatically increased fouling resistance and maintains a clean surface (h). Relative fouling indices, F_1 (b,f) – the fraction of surface coverage for the coated surface compared to the bare glass control – and F_2 (c,g) – the fraction of surface coverage in the presence of chlorination, compared to that in the absence of chlorination for a bare glass surface – are used to quantify the effects of coating and chlorination, respectively. The synergistic fouling prevention is quantified by the synergistic index, S (d,h), where $S < 1$ indicates synergy between the coating and chlorination. See also Supporting Information, Movies 3 and 4. Images in (a-h) are captured with the same magnification and the scale bar represents 50 μm . i-q, Comparison of the attachment and proliferation of a *V. cyclitrophicus* bacterium on (i,l,o) a bare surface, (j,m,p) a bare surface with chlorination, and (k,n,q) a coated surface with chlorination. The 5 ppm chlorine addition did not prevent bacterial proliferation on the surface (m,n,p). The zwitterionic chemistry is critical for the synergistic fouling resistance, as bacteria are readily removed from the zwitterion-coated surface by even laminar flow (Reynolds number ~ 0.1) (q). See also Supporting Information, Movie 5. The scale bar represents 5 μm .

velocity of $\sim 560 \mu\text{m s}^{-1}$). Fabrication of multiple (2-4) microchannels on the same chip allows parallel, simultaneous experiments and thus a direct comparison of different treatments and the minimization of confounding factors. Because experiments lasting up to 100 hours reveal no discernible surface attachment (Supporting Information, Figure S7; Supporting Information, Movies 1 and 2), irrespective of surface conditions, we run accelerated fouling experiments with concentrated cultures of *V. cyclitrophicus*, grown overnight in artificial seawater and concentrated to an optical density ($\text{OD}_{600} = 0.2$; $\sim 2 \times 10^8$ cells ml^{-1}) corresponding to early exponential phase. This bacterial concentration is ~ 200 times that of typical seawater.

In the accelerated tests, the iCVD zwitterionic coatings show much greater resistance to bacterial attachment than bare glass (Figure 3a,b,e,f; Supporting Information, Figure S8; Supporting Information, Movie 3). Fouling is quantified by time-lapse imaging of the surface, followed by image analysis to determine the number of attached cells and the percent surface coverage by bacteria. As the variables are time-dependent, the behavior at 5 hours and 12 hours will be discussed, but general conclusions apply also to the data at other times. Despite the intrinsic fouling resistance of glass surfaces,^[26] the number of attached cells on bare glass increases steadily over time, and exponentially after 50 minutes. After 5 hours,

the cell count over a 0.16-mm² area of the bare glass surface reaches ~7500, (Figure 3a), whereas it remains close to zero on the coated surface (Figure 3b). Defining a relative fouling index, F_1 , as the fraction of surface coverage for the coated surface compared to the bare glass control, we find that F_1 decreases drastically over time for functionalized copolymer 1 and drops to ~0.01 after 5 hours (Supporting Information, Figure S8). This result demonstrates the exceptional fouling resistance of iCVD zwitterionic coatings, in particular in view of the fact that smooth, bare glass is already a rather good anti-fouling surface.^[26]

The surfaces' antifouling effects are further boosted by low-level chlorination, resulting in a new synergistic approach against fouling made possible by functionalized copolymer 1's good resistance to chlorine (Figure 2a,e,f). We run additional, accelerated microfluidic tests where the suspension of *V. cyclitrophicus* is amended with 5 ppm of sodium hypochlorite (Figure 3c,d,g,h; Supporting Information, Movie 4), a concentration comparable to the residual chlorine level in the USA national drinking water standards.^[30] To quantify the effect of chlorination we define a second fouling index, F_2 , computed as the fraction of surface coverage in the presence of chlorination, compared to that in the absence of chlorination, for the case of a bare glass surface. Although chlorination overall reduces surface fouling, signs of fouling on bare glass in the presence of 5 ppm chlorine emerge after 5 hours ($F_2 \sim 0.45$; Figure 3c) and after 12 hours fouling is severe ($F_2 \sim 0.58$; Figure 3g). Therefore, chlorination at a level of 5 ppm is less effective than the zwitterionic coating in preventing bacterial attachment. However, the synergistic effect of the zwitterionic coating and chlorination dramatically increases fouling resistance over each treatment in isolation (Figure 3d,h). After 12-hour exposure to the *V. cyclitrophicus* suspension, the surface coverage is $35.3 \pm 1.7\%$ on bare glass in the presence of 5 ppm chlorine ($F_2 \sim 0.58$), $14.1 \pm 3.4\%$ on the coated surface without chlorine ($F_1 \sim 0.14$), and only $1.5 \pm 0.4\%$ on the coated surface in the presence of 5 ppm chlorine. The percent surface coverage in the synergistic treatment is 0.02 of that of a bare glass surface without chlorine, four-fold smaller than the prediction ($F_1 \times F_2$) obtained if the effect was simply multiplicative.

To quantify the synergistic effect of the two antifouling strategies, we compute an antifouling synergistic index, S (Figure 4a, inset). Synergistic indices have been used among others to describe the effects of multi-strategy anti-tumor treatments, where $S < 1$ indicates a synergistic effect in killing tumor cells by the different strategies in the treatment.^[31,32] Here we define S as

$$S = \frac{\% \text{Surface coverage}_{\text{combination treatment, observed}}}{\% \text{Surface coverage}_{\text{combination treatment, expected}}} = \frac{\% \text{Surface coverage}_{\text{combination treatment, observed}}}{F_1 \times F_2 \times \% \text{Surface coverage}_{\text{bare glass}}} \quad (1)$$

The temporal dynamics of S (Figure 4a, inset) reveal values of $S < 1$ after ~400 minutes, and a subsequent steady decrease to ~0.1 after 900 minutes. No signs of saturation in the decrease are observed, demonstrating the long-term nature of the synergy. Values of S over the first 5 hours are not reported because the surface chemistry alone reduces fouling to non-detectable

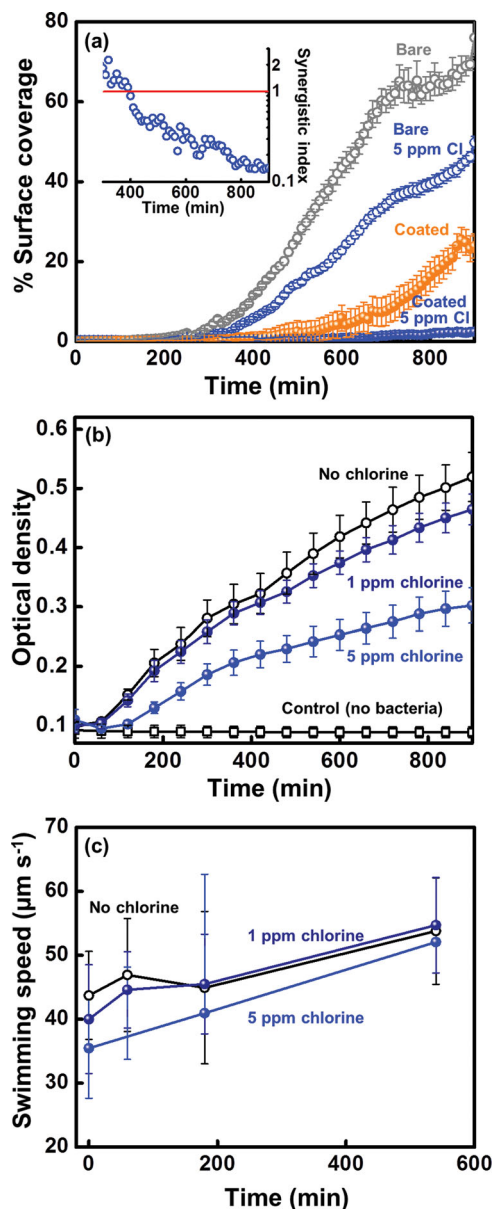


Figure 4. Synergistic prevention of bacterial fouling by the combination treatment. a) Surface coverage by *V. cyclitrophicus* bacteria under different conditions. The synergistic treatment – integrating iCVD zwitterionic coating with low-level (5 ppm) chlorination – shows exceptional long-term antifouling activity even under accelerated biofouling conditions (i.e., dense bacterial suspensions), when each method in isolation begins to fail. *Inset:* Time series of the synergistic index (S), quantifying synergistic effect of the two antifouling strategies. Values of $S < 1$ indicate a positive synergy between the two treatments. The monotonic decrease of S , with no signs of saturation after 15 hours, demonstrates the importance of synergistic effect on long-term fouling resistance. b) Viability of *V. cyclitrophicus* upon addition of chlorine at different concentrations. 1 ppm chlorine does not significantly impact bacterial growth, whereas 5 ppm chlorine reduces the optical density by 42%, but does not kill bacteria. Killing by chlorine is thus not the dominant factor in the success of the synergistic treatment. c) Mean swimming speed of *V. cyclitrophicus*, obtained by tracking of individual cells. Addition of up to 5 ppm chlorine does not significantly change the bacteria's swimming speed, suggesting that prevention of attachment is not due to a reduction of encounter rates with surfaces.

levels (i.e., $F_1 \sim 0$) during this time and thus the quantification of S is not meaningful.

In the attempt to reveal the mechanism underpinning the synergistic effect, the cell-surface interaction is investigated by observing a single bacterium for its proliferation and motility on the surface for the different treatments (Figure 3i-q; Supporting Information, Movie 5). After 85 minutes, replication has occurred under all conditions (Figure 3l-n), at a mildly lower rate in the presence of 5 ppm chlorine (Figure 3m,n), suggesting that the low dose of chlorine has only small effects on cell growth. This hypothesis is supported by direct viability tests (Figure 4b), showing that the growth of *V. cyclitrophicus* (measured as the optical density of cell cultures) is negligibly affected by addition of 1 ppm chlorine and exhibits a 42% reduction with 5 ppm chlorine addition. Furthermore, tracking of individual cells shows that motility is not significantly affected by 1 ppm or 5 ppm chlorination (Figure 4c). Although growth in batch culture might differ from growth on a microchannel surface, taken together these results (Figures 4b and 3l-n) demonstrate that the observed antifouling and synergistic effect of chlorine are not based on killing of the bacteria. Instead, the primary difference among the three single-cell cases (Figure 3i-q) resides in the dependence of cell removal from the surface on the surface chemistry (Figure 3o-q): whereas bacteria remain largely attached to the bare glass surface, they are easily removed from the coated surface by ambient fluid flow, independent of the presence of chlorine. In particular, bacterial removal from the iCVD zwitterionic coating occurs readily even under the low, laminar flow conditions within the microchannel (Reynolds number ~ 0.1).

We have demonstrated the ability of ultrathin, chlorine-resistant iCVD zwitterionic copolymers to act as antifouling coatings and, based on their resistance to chlorine, we have proposed a novel, multi-strategy approach to antifouling, which hinges on the synergy between surface chemistry and chlorination. The zwitterionic coating prevents the attachment of *V. cyclitrophicus* almost 100 times more effectively than glass after 5 hours (Figures 3a,b and 4a; Supporting Information, Figure S8), while chlorination, with concentrations as low as the regulated chlorine residue in drinking water, is able to enhance the long-term fouling resistance of the zwitterionic coating by 9.4-fold after 12 hours (Figures 3d,h and 4a), with no signs of saturation.

A key advantage of the zwitterionic coatings reported here is the substrate-independence of the vapor application process, which makes these coatings easily applicable to a broad range of surfaces. In particular, these coatings may be applied on the latest salt-rejecting layers,^[15–17] which resist exposure to chlorine, providing a path towards solving the desalination industry's bottleneck of the susceptibility of TFC-RO membranes to oxidative damage by chlorine. The surface treatment is benign, easily scalable^[33] and compatible with the infrastructure in membrane industry,^[2] which gives rise to a stable, non-toxic and inexpensive ultrathin coating. The good fouling resistance and chlorine resistance of this coating can help eliminate the most energy- and chemical-intensive step (pretreatment of seawater) in a RO desalination plant,^[2] and reduce the environmental impacts of brine discharge. This approach therefore promises to lower the price of freshwater in water-scarce countries, where

desalination may serve as the only viable means to provide the water supply necessary to sustain agriculture, support personal consumption, and promote economic development.

Experimental Section

Film Deposition and Derivatization: All iCVD films were deposited in a custom-built vacuum reactor (Sharon Vacuum), as previously described.^[9,10] All the chemicals were used as purchased without further purification. Silicon (Si) wafers (Wafer World, test grade) were coated with P4VP or the copolymer of 4VP and DVB without pre-treatment. Prior to deposition, commercial RO membranes (Koch Membrane System, TFC-HR) were cleaned with filtered nitrogen, and then treated with oxygen plasma for 1 minute and then placed in the reactor chamber. The glass slides were treated with trichlorovinylsilane (Aldrich, 97%), as described previously.^[34] During iCVD depositions, 4VP (Aldrich, 95%) and DVB (Aldrich, 80%) monomers were heated up to 50 °C and 65 °C in glass jars, respectively and delivered into the reactor using mass flow controllers (1150 MFC, MKS Instruments). Argon patch flow was metered into the reactor through a mass flow controller (1479 MFC, MKS Instruments) and the flow rate was varied to keep the residence time constant. Systematic variation of the flow rate ratios of the two monomers was performed to yield high-zwitterionic-percentage, yet chlorine-resistant films of poly(4-vinylpyridine-co-divinylbenzene) (PVD). Films were deposited at a filament temperature of 250 °C and a stage temperature of 20 °C. Total pressure in the vacuum chamber was maintained at 0.8 Torr for all depositions.

In situ interferometry with a 633 nm HeNe laser source (JDS Uniphase) was used to monitor the film growth and deposit desired thicknesses on Si substrates. A more accurate film thickness on the Si wafer substrates was measured post-deposition using a J.A. Woollam M-2000 spectroscopic ellipsometry at three different incidence angles (65°, 70°, 75°) using 190 wavelengths from 315 to 718 nm. The data were fit using a Cauchy-Urbach model. After deposition, the PVD-coated substrates were derivatized as reported previously.^[9,10] FTIR, XPS and contact angle measurements were performed as described previously.^[9,10]

Permeation and Salt Rejection Tests: Tests of the coated/bare membranes were performed using a commercial dead-end membrane filtration unit (Sterlitech Corp., HP4750) with a nitrogen cylinder to supply feed pressure, which was kept at 700 psi for all tests. The flow rates of the permeate were determined using a 100 ml metered flask. For the salt rejection tests, 35000 ppm sodium chloride dissolved in deionized water was used as feed solution. A conductivity meter (CDH-152, Omega Engineering Inc.) was used to measure the conductivities of the feed and permeate to calculate the salt rejection.

Chlorine Resistance Tests: Samples subject to chlorine resistance tests were soaked in deionized water for 2 hours, to remove the surface absorbed PS molecules and loosely attached oligomers of 4VP. Samples were dried with nitrogen gas and soaked in aqueous solution of sodium hypochlorite with the concentration of 1000 ppm for various treatment durations. FTIR spectra and dynamic contact angle measurements were taken before and after treating with chlorine solutions.

Bacterial Adhesion Tests: *V. cyclitrophicus* was used as the model microorganism. Bacteria cells from freezer stocks were inoculated and grown overnight in artificial seawater at 30 °C to an optical density (OD₆₀₀) of 1 while agitated on a shaker (150 rpm). Cells were suspended in fresh artificial seawater and incubated at 37 °C on a shaker (180 rpm) until the optical density reached 0.2. The bacterial solution was then injected into the microfluidic channels at a constant flow rate of 2 $\mu\text{l min}^{-1}$, which corresponds to an average flow velocity of 560 $\mu\text{m s}^{-1}$. During the combination treatment, chlorine was directly added to the vessel containing the media with bacteria to a final concentration of 5 ppm. Note that in this case the images (Figure 3) acquired at a certain time (t hours) captured bacteria that have been exposed to chlorine for t h.

Supporting Information

Supporting Information is available from the Wiley Online Library or from the author.

Acknowledgements

The authors thank the support from DOE Office of ARPA-E under award AR0000294 and the King Fahd University of Petroleum and Minerals in Dhahran, Saudi Arabia, for funding the research reported in this paper through the Center for Clean Water and Clean Energy at MIT and KFUPM (to K.K.G.) as well as support through NSF grants OCE-6917641-CAREER and CBET-6923975, and NIH grant 6917755 (to R.S.). Dr. Hongchul Jang has been partially supported by a Samsung Fellowship. We thank Jonathan Shu from the Cornell Center for Materials Research (CCMR) for help with XPS measurements.

Received: August 31, 2013

Revised: October 16, 2013

Published online: December 27, 2013

- [1] WHO Book 10 facts about water scarcity, <http://www.who.int/features/factfiles/water/en/>.
- [2] M. Elimelech, W. A. Phillip, *Science* **2011**, *333*, 712–717.
- [3] S. Jiang, Z. Cao, *Adv. Mater.* **2010**, *22*, 920–932.
- [4] L. Zhang, Z. Cao, T. Bai, L. Carr, J.-R. Ella-Menye, C. Irvin, B. D. Ratner, S. Jiang, *Nat. Biotechnol.* **2013**, *31*, 553–556.
- [5] S. Chen, J. Zheng, L. Li, S. Jiang, *J. Am. Chem. Soc.* **2005**, *127*, 14473–14478.
- [6] H. Kitano, T. Mori, Y. Takeuchi, S. Tada, M. Gemmei-Ide, Y. Yokoyama, M. Tanaka, *Macromol. Biosci.* **2005**, *5*, 314–321.
- [7] R. Quintana, M. Gosa, D. J. czewski, E. Kutnyanszky, G. J. Vancso, *Langmuir* **2013**.
- [8] J. S. Louie, I. Pinnau, M. Reinhard, *J. Membr. Sci.* **2011**, *367*, 249–255.
- [9] R. Yang, J. Xu, G. Ozaydin-Ince, S. Y. Wong, K. K. Gleason, *Chem. Mater.* **2011**, *23*, 1263–1272.
- [10] R. Yang, K. K. Gleason, *Langmuir* **2012**, *28*, 12266–12274.
- [11] G. Ozaydin-Ince, A. Matin, Z. Khan, S. M. J. Zaidi, K. K. Gleason, *Thin Solid Films* **2013**, *539*, 181–187.
- [12] H. B. Park, B. D. Freeman, Z.-B. Zhang, M. Sankir, J. E. McGrath, *Angew. Chem. Int. Ed.* **2008**, *47*, 6019–6024.
- [13] C. D. Petruczok, R. Yang, K. K. Gleason, *Macromolecules* **2013**, *46*, 1832–1840.
- [14] M. E. Alf, A. Asatekin, M. C. Barr, S. H. Baxamusa, H. Chelawat, G. Ozaydin-Ince, C. D. Petruczok, R. Sreenivasan, W. E. Tenhaeff, N. J. Trujillo, S. Vaddiraju, J. Xu, K. K. Gleason, *Adv. Mater.* **2010**, *22*, 1993–2027.
- [15] D. Cohen-Tanugi, J. C. Grossman, *Nano Lett.* **2012**, *12*, 3602–3608.
- [16] M. Majumder, N. Chopra, R. Andrews, B. J. Hinds, *Nature* **2005**, *438*, 44.
- [17] J. K. Holt, H. G. Park, Y. Wang, M. Stadermann, A. B. Artyukhin, C. P. Grigoropoulos, A. Noy, O. Bakajin, *Science* **2006**, *312*, 1034–1037.
- [18] F. Natalio, R. Andre, A. F. Hartog, B. Stoll, K. P. Jochum, R. Wever, W. Tremel, *Nat. Nanotechnol.* **2012**, *7*, 530–535.
- [19] D. Rana, T. Matsuura, *Chem. Rev.* **2010**, *110*, 2448–2471.
- [20] G. Beamson, D. Briggs, in *High Resolution XPS of Organic Polymers: the Scienta ESCA300 Data Base*, John Wiley & Sons, New York **1992**.
- [21] C. G. Spanos, J. P. S. Badyal, A. J. Goodwin, P. J. Merlin, *Polymer* **2005**, *46*, 8908–8912.
- [22] A. S. Goldmann, A. Walther, L. Nebhani, R. Joso, D. Ernst, K. Loos, C. Barner-Kowollik, L. Barner, A. H. E. Müller, *Macromolecules* **2009**, *42*, 3707–3714.
- [23] L. Wang, Z. Wang, X. Zhang, J. Shen, L. Chi, H. Fuchs, *Macromol. Rapid Commun.* **1997**, *18*, 509–514.
- [24] D. Lin-Vien, N. Colthup, B. W. Fateley, G. J. Grasselli, in *The Handbook of Infrared and Raman Characteristic Frequencies of Organic Molecules*, Academic Press, San Diego **1991**.
- [25] R. J. Good, *J. Adhes. Sci. Technol.* **1992**, *6*, 1269–1302.
- [26] C. J. Weinman, N. Gunari, S. Krishnan, R. Dong, M. Y. Paik, K. E. Sohn, G. C. Walker, E. J. Kramer, D. A. Fischer, C. K. Ober, *Soft Matter* **2010**, *6*, 3237–3243.
- [27] S. H. Baxamusa, K. K. Gleason, *Adv. Funct. Mater.* **2009**, *19*, 3489–3496.
- [28] A. Asatekin, A. Mennitti, S. Kang, M. Elimelech, E. Morgenroth, A. M. Mayes, *J. Membr. Sci.* **2006**, *285*, 81–89.
- [29] R. Stocker, J. R. Seymour, A. Samadani, D. E. Hunt, M. F. Polz, *Proc. Natl. Acad. Sci. USA* **2008**, *105*, 4209–4214.
- [30] EPA Drinking Water Contaminants, <http://water.epa.gov/drink/contaminants/index.cfm>.
- [31] Z. Zhang, J. C. Lee, L. Lin, V. Olivas, V. Au, T. LaFramboise, M. Abdel-Rahman, X. Wang, A. D. Levine, J. K. Rho, Y. J. Choi, C.-M. Choi, S.-W. Kim, S. J. Jang, Y. S. Park, W. S. Kim, D. H. Lee, J.-S. Lee, V. A. Miller, M. Arcila, M. Ladanyi, P. Moonsamy, C. Sawyers, T. J. Boggon, P. C. Ma, C. Costa, M. Taron, R. Rosell, B. Halmos, T. G. Bivona, *Nat. Genet.* **2012**, *44*, 852–860.
- [32] C. T. Keith, A. A. Borisy, B. R. Stockwell, *Nat. Rev. Drug Discov.* **2005**, *4*, 71–78.
- [33] M. Gupta, K. K. Gleason, *Thin Solid Films* **2006**, *515*, 1579–1584.
- [34] N. J. Trujillo, S. H. Baxamusa, K. K. Gleason, *Chem. Mater.* **2009**, *21*, 742–750.